

# Spin-polarized currents in superconducting films

M. Božović\* and Z. Radović†

*Department of Physics, University of Belgrade, P.O. Box 368, 11001 Belgrade, Yugoslavia*

We present a microscopic theory of coherent quantum transport through a superconducting film between two ferromagnetic electrodes. The scattering problem is solved for the general case of ferromagnet/superconductor/ferromagnet (FSF) double-barrier junction, including the interface transparency from metallic to tunnel limit, and the Fermi velocity mismatch. Charge and spin conductance spectra of FSF junctions are calculated for parallel (P) and antiparallel (AP) alignment of the electrode magnetization. Limiting cases of nonmagnetic normal-metal electrodes (NSN) and of incoherent transport are also presented. We focus on two characteristic features of finite size and coherency: subgap tunneling of electrons, and oscillations of the differential conductance. Periodic vanishing of the Andreev reflection at the energies of geometrical resonances above the superconducting gap is a striking consequence of the quasiparticle interference. Also, the non-trivial spin-polarization of the current is found for FSF junctions in AP alignment. This is in contrast with the incoherent transport, where the unpolarized current is accompanied by excess spin accumulation and destruction of superconductivity. Application to spectroscopic measurements of the superconducting gap and the Fermi velocity is also discussed.

## I. INTRODUCTION

During the past decade, there has been a growing interest in various electronic systems driven out of equilibrium by the injection of spin-polarized carriers. Such systems can be realized by current-biasing structures consisting of ferromagnetic and non-ferromagnetic (e.g. superconducting) layers, due to the difference in population of majority and minority spin subbands.<sup>1</sup> The concept of spin-polarized current nowadays has attracted considerable interest in ferromagnetic heterostructures, in particular for applications in spintronics.<sup>2</sup>

Charge transport through a normal metal/superconductor (NS) junction, with an insulating barrier of arbitrary strength at the interface, has been studied by Blonder, Tinkham, and Klapwijk (BTK),<sup>3</sup> and the Andreev reflection is recognized as the mechanism of normal-to-supercurrent conversion.<sup>4,5</sup> The BTK theory has been extended by Tanaka and Kashiwaya to include the anisotropy of the pair potential in  $d$ -wave superconductors.<sup>6,7</sup> The modification of the Andreev reflection by the spin injection from a ferromagnetic metal into a superconductor in ferromagnet/superconductor (FS) junctions was first analyzed by de Jong and Beenakker.<sup>8</sup> More recently, the effects of unconventional  $d$ -wave and  $p$ -wave pairing and of the exchange interaction in FS systems, such as the zero-bias conductance peak and the virtual Andreev reflection, have been clarified by Kashiwaya *et al.*<sup>9</sup> and Yoshida *et al.*<sup>10</sup> The Fermi velocity mismatch between two metals can also significantly affect the Andreev reflection by altering the subgap conductance,<sup>11</sup> which is similar to the presence of an insulating barrier.<sup>12</sup>

In experiments, a superconductor is used to determine the spin polarization of the current injected from (or into) a ferromagnet by measuring the differential conductance. These measurements have been performed on tunnel junctions in an external magnetic field,<sup>13,14</sup> metallic point contacts,<sup>15,16</sup> nano-contacts formed by microlithography,<sup>17</sup> and FS junctions with  $d$ -wave superconductors, grown by molecular beam epitaxy.<sup>18</sup> In diffusive FS junctions, the excess resistance may be induced by spin accumulation near the insulating interface,<sup>19</sup> and by the proximity effect.<sup>20,21,22</sup> When electrons pass incoherently through the interfaces, the BTK model can be successfully applied to normal metal/superconductor/normal metal (NSN) or ferromagnet/superconductor/ferromagnet (FSF) double junctions.<sup>23,24</sup> However, the properties of coherent quantum transport in clean superconducting heterostructures are strongly influenced by size effects, which are not included in the BTK model. Well-known examples are the current-carrying Andreev bound states<sup>7,25</sup> and multiple Andreev reflections<sup>26,27,28</sup> in superconductor/normal metal/superconductor (SNS) junctions. Since early experiments by Tomasch,<sup>29</sup> the geometric resonance nature of the differential conductance oscillations in SNS and NSN tunnel junctions has been ascribed to the electron interference in the central film.<sup>30,31,32,33</sup> Recently, the McMillan-Rowell oscillations were observed in SNS edge junctions of  $d$ -wave superconductors, and used for measurements of the superconducting gap and the Fermi velocity.<sup>34</sup>

Here we present a comprehensive microscopic theory of coherent transport in FSF double junctions (with NSN as a special case).<sup>35,36</sup> We limit ourselves to clean conventional ( $s$ -wave) superconductors, and neglect, for simplicity, the self-consistency of the pair potential,<sup>37,38</sup> and nonequilibrium effects of charge and spin accumulation at the

---

\* E-mail: mbozovic@infosky.net

† E-mail: zradovic@ff.bg.ac.yu

interfaces.<sup>39,40</sup> When two interfaces are recognized by electrons simultaneously, characteristic features of finite size and coherency are the subgap tunneling of electrons and oscillations of both charge and spin differential conductances above the gap. One consequence of the quasiparticle interference is the periodic vanishing of the Andreev reflection at the energies of geometrical resonances. The other is the existence of a non-trivial spin-polarization of the current not only for the parallel (P), but also for the antiparallel (AP) alignment of the electrode magnetizations. Previous analysis of incoherent transport in FSF double junctions predict the absence of the spin current and suppression of superconductivity with increasing voltage for AP alignment, as a result of spin imbalance in the superconducting film.<sup>23,24</sup>

## II. THE SCATTERING PROBLEM

We consider an FSF double junction consisting of a clean superconducting layer of thickness  $l$ , connected to ferromagnetic electrodes by thin, insulating interfaces, Fig. 1. For the ferromagnetic metal we adopt the Stoner model describing the spin-polarization effect by the usual one-electron Hamiltonian with an exchange potential. The quasiparticle propagation is described by the Bogoliubov-de Gennes equation

$$\begin{pmatrix} H_0(\mathbf{r}) - \rho_\sigma h(\mathbf{r}) & \Delta(\mathbf{r}) \\ \Delta^*(\mathbf{r}) & -H_0(\mathbf{r}) + \rho_{\bar{\sigma}} h(\mathbf{r}) \end{pmatrix} \Psi_\sigma(\mathbf{r}) = E \Psi_\sigma(\mathbf{r}), \quad (1)$$

with  $H_0(\mathbf{r}) = -\hbar^2 \nabla^2 / 2m + W(\mathbf{r}) + U(\mathbf{r}) - \mu$ , where  $U(\mathbf{r})$  and  $\mu$  are the Hartree and the chemical potential, respectively. The interface potential is modeled by  $W(\mathbf{r}) = \hat{W} \{ \delta(z) + \delta(z-l) \}$ , where  $z$ -axis is perpendicular to the layers and  $\delta(z)$  is the Dirac  $\delta$ -function. Neglecting the self-consistency of the superconducting pair potential,  $\Delta(\mathbf{r})$  is taken in the form  $\Delta \Theta(z) \Theta(l-z)$ , where  $\Delta$  is the bulk superconducting gap and  $\Theta(z)$  is the Heaviside step function. In Eq. (1),  $\sigma$  is the quasiparticle spin ( $\sigma = \uparrow, \downarrow$  and  $\bar{\sigma} = \downarrow, \uparrow$ ),  $E$  is the energy with respect to  $\mu$ ,  $h(\mathbf{r})$  is the exchange potential given by  $h_0 \{ \Theta(-z) + [-] \Theta(z-l) \}$  for the P [AP] alignment, and  $\rho_\sigma$  is 1 (-1) for spins up (down). The electron effective mass  $m$  is assumed to be the same for the whole junction. Here,  $\mu - U(\mathbf{r})$  is the Fermi energy of the superconductor,  $E_F^{(S)}$ , or the mean Fermi energy of a ferromagnet,  $E_F^{(F)} = (E_F^\uparrow + E_F^\downarrow)/2$ . Moduli of the Fermi wave vectors,  $k_F^{(F)} = \sqrt{2mE_F^{(F)}/\hbar^2}$  and  $k_F^{(S)} = \sqrt{2mE_F^{(S)}/\hbar^2}$ , can be different in general, and in the following, the Fermi wave vector mismatch (FWVM) will be taken into account through the parameter  $\kappa = k_F^{(F)}/k_F^{(S)}$ . The parallel component of the wave vector  $\mathbf{k}_{\parallel, \sigma}$  is conserved, and the wave function

$$\Psi_\sigma(\mathbf{r}) = \exp(i\mathbf{k}_{\parallel, \sigma} \cdot \mathbf{r}) \psi_\sigma(z), \quad (2)$$

satisfies the boundary conditions

$$\psi_\sigma(z)|_{z=0_-} = \psi_\sigma(z)|_{z=0_+}, \quad (3)$$

$$\left. \frac{d\psi_\sigma(z)}{dz} \right|_{z=0_-} = \left. \frac{d\psi_\sigma(z)}{dz} \right|_{z=0_+} - \frac{2m\hat{W}}{\hbar^2} \psi_\sigma(0), \quad (4)$$

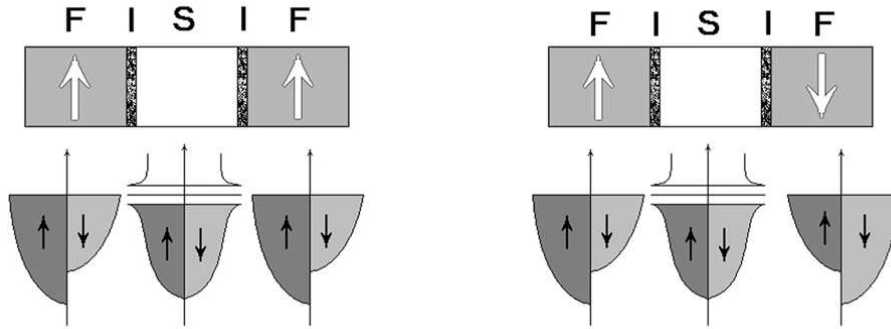


FIG. 1: Double barrier junction consisting of two ferromagnets (F) and a superconductor (S) separated by insulating barriers (I), for parallel (left panel) and antiparallel (right panel) alignment of the electrode magnetization. Schematic of the corresponding densities of states.

$$\psi_\sigma(z)|_{z=l_-} = \psi_\sigma(z)|_{z=l_+}, \quad (5)$$

$$\left. \frac{d\psi_\sigma(z)}{dz} \right|_{z=l_-} = \left. \frac{d\psi_\sigma(z)}{dz} \right|_{z=l_+} - \frac{2m\hat{W}}{\hbar^2} \psi_\sigma(l). \quad (6)$$

Four independent solutions of Eq. (1) correspond to the four types of injection: an electron or a hole from either the left or from the right electrode.<sup>5</sup>

For the injection of an electron from the left, with energy  $E > 0$ , spin  $\sigma$ , and angle of incidence  $\theta$  (measured from the  $z$ -axis), solution for  $\psi_\sigma(z)$  in various regions has the following form: in the left ferromagnet ( $z < 0$ )

$$\psi_\sigma(z) = \{\exp(ik_\sigma^+ z) + b_\sigma(E, \theta) \exp(-ik_\sigma^+ z)\} \begin{pmatrix} 1 \\ 0 \end{pmatrix} + a_\sigma(E, \theta) \exp(ik_{\bar{\sigma}}^- z) \begin{pmatrix} 0 \\ 1 \end{pmatrix}, \quad (7)$$

in the superconductor ( $0 < z < l$ )

$$\begin{aligned} \psi_\sigma(z) = & \{c_1(E, \theta) \exp(iq_\sigma^+ z) + c_2(E, \theta) \exp(-iq_\sigma^+ z)\} \begin{pmatrix} \bar{u} \\ \bar{v} \end{pmatrix} \\ & + \{c_3(E, \theta) \exp(iq_\sigma^- z) + c_4(E, \theta) \exp(-iq_\sigma^- z)\} \begin{pmatrix} \bar{v}^* \\ \bar{u}^* \end{pmatrix}, \end{aligned} \quad (8)$$

and in the right ferromagnet ( $z > l$ ), for the P [AP] alignment of the magnetizations

$$\psi_\sigma(z) = c_\sigma(E, \theta) \exp(ik_{\sigma[\bar{\sigma}]}^+ z) \begin{pmatrix} 1 \\ 0 \end{pmatrix} + d_\sigma(E, \theta) \exp(-ik_{\sigma[\sigma]}^- z) \begin{pmatrix} 0 \\ 1 \end{pmatrix}. \quad (9)$$

Here,  $\bar{u} = \sqrt{(1 + \Omega/E)/2}$  and  $\bar{v} = \sqrt{(1 - \Omega/E)/2}$  are the BCS coherence factors, and  $\Omega = \sqrt{E^2 - \Delta^2}$ . The  $z$ -components of the wave vectors are  $k_\sigma^\pm = \sqrt{(2m/\hbar^2)(E_F^{(F)} + \rho_\sigma h_0 \pm E) - \mathbf{k}_{||,\sigma}^2}$ , and  $q_\sigma^\pm = \sqrt{(2m/\hbar^2)(E_F^{(S)} \pm \Omega) - \mathbf{k}_{||,\sigma}^2}$ , where  $|\mathbf{k}_{||,\sigma}| = \sqrt{(2m/\hbar^2)(E_F^{(F)} + \rho_\sigma h_0 + E) \sin^2 \theta}$ . The coefficients  $a_\sigma$ ,  $b_\sigma$ ,  $c_\sigma$ , and  $d_\sigma$  are, respectively, the probability amplitudes of: (1) Andreev reflection as a hole of the opposite spin (AR); (2) normal reflection as an electron (NR); (3) transmission to the right electrode as an electron (TE); (4) transmission to the right electrode as a hole of the opposite spin (TH). Processes (1) and (4) are equivalent to the formation of a Cooper pair in the superconductor by taking one more electron from either the left or the right electrode, respectively. Amplitudes of the Bogoliubov electron-like and hole-like quasiparticles, propagating in the superconducting layer, are given by the coefficients  $c_1$  through  $c_4$ .

From the probability current conservation, the probabilities of outgoing particles satisfy the normalization condition

$$A_\sigma(E, \theta) + B_\sigma(E, \theta) + C_\sigma(E, \theta) + D_\sigma(E, \theta) = 1, \quad (10)$$

where,

$$A_\sigma(E, \theta) = \Re \left( \frac{\tilde{k}_{\bar{\sigma}}}{\tilde{k}_\sigma} \right) |a_\sigma(E, \theta)|^2, \quad (11)$$

$$B_\sigma(E, \theta) = |b_\sigma(E, \theta)|^2, \quad (12)$$

$$C_\sigma(E, \theta) = \Re \left( \frac{\tilde{k}_{\sigma[\bar{\sigma}]}}{\tilde{k}_\sigma} \right) |c_\sigma(E, \theta)|^2, \quad (13)$$

$$D_\sigma(E, \theta) = \Re \left( \frac{\tilde{k}_{\bar{\sigma}[\sigma]}}{\tilde{k}_\sigma} \right) |d_\sigma(E, \theta)|^2. \quad (14)$$

Neglecting small terms  $E/E_F^{(F)} \ll 1$  and  $\Delta/E_F^{(S)} \ll 1$  in the wave vectors, except in the exponents

$$\zeta_\pm = l (q_\sigma^+ \pm q_\sigma^-), \quad (15)$$

solutions of Eqs. (3)-(6) for the probability amplitudes can be written in the following form

$$a_\sigma(E, \theta) = \frac{4(\tilde{k}_\sigma/\tilde{q}_\sigma)\Delta \sin(\zeta_-/2)}{\Gamma} [\mathcal{A}_+^R E \sin(\zeta_-/2) + i\mathcal{B}_+^R \Omega \cos(\zeta_-/2)], \quad (16)$$

$$b_\sigma(E, \theta) = \frac{1}{\Gamma} [\mathcal{A}_+^R \mathcal{C}_+ \Delta^2 - (\mathcal{A}_+^R \mathcal{C}_+ E^2 + \mathcal{B}_+^R \mathcal{D}_+ \Omega^2) \cos(\zeta_-) + (\mathcal{A}_-^R \mathcal{C}_- + \mathcal{B}_-^R \mathcal{D}_-) \Omega^2 \cos(\zeta_+) + i (\mathcal{B}_+^R \mathcal{C}_+ + \mathcal{A}_+^R \mathcal{D}_+) E \Omega \sin(\zeta_-) - i (\mathcal{B}_-^R \mathcal{C}_- + \mathcal{A}_-^R \mathcal{D}_-) \Omega^2 \sin(\zeta_+)], \quad (17)$$

$$c_\sigma(E, \theta) = \frac{4(\tilde{k}_\sigma/\tilde{q}_\sigma)\Omega e^{-ik_\sigma^+ l}}{\Gamma} \times \times \{i [\mathcal{F}_+ \cos(\zeta_+/2) + i\mathcal{E}_+ \sin(\zeta_+/2)] E \sin(\zeta_-/2) - [\mathcal{E}_+ \cos(\zeta_+/2) + i\mathcal{F}_+ \sin(\zeta_+/2)] \Omega \cos(\zeta_-/2)\}, \quad (18)$$

$$d_\sigma(E, \theta) = \frac{4(\tilde{k}_\sigma/\tilde{q}_\sigma)\Delta\Omega e^{ik_\sigma^- l}}{\Gamma} \times \times i [\mathcal{F}_- \cos(\zeta_+/2) + i\mathcal{E}_- \sin(\zeta_+/2)] \sin(\zeta_-/2), \quad (19)$$

where

$$\Gamma = \mathcal{A}_+^L \mathcal{A}_+^R \Delta^2 - (\mathcal{A}_+^L \mathcal{A}_+^R E^2 + \mathcal{B}_+^L \mathcal{B}_+^R \Omega^2) \cos(\zeta_-) + (\mathcal{A}_-^L \mathcal{A}_-^R + \mathcal{B}_-^L \mathcal{B}_-^R) \Omega^2 \cos(\zeta_+) + i (\mathcal{A}_+^L \mathcal{B}_+^R + \mathcal{B}_+^L \mathcal{A}_+^R) E \Omega \sin(\zeta_-) - i (\mathcal{A}_-^L \mathcal{B}_-^R + \mathcal{B}_-^L \mathcal{A}_-^R) \Omega^2 \sin(\zeta_+). \quad (20)$$

In Eqs. (16)-(20)

$$\begin{aligned} \mathcal{A}_\pm^{L(R)} &= K_1^{L(R)} \pm K_2^{L(R)}, & \mathcal{B}_\pm^{L(R)} &= 1 \pm K_1^{L(R)} K_2^{L(R)}, & \mathcal{C}_\pm &= K_1^{L*} \mp K_2^L, \\ \mathcal{D}_\pm &= -(1 \mp K_1^{L*} K_2^L), & \mathcal{E}_\pm &= K_2^L \pm K_2^R, & \mathcal{F}_\pm &= 1 \pm K_2^L K_2^R, \end{aligned}$$

with  $K_1^L = (\tilde{k}_\sigma + iZ)/\tilde{q}_\sigma$ ,  $K_2^L = (\tilde{k}_\sigma - iZ)/\tilde{q}_\sigma$ ,  $K_1^R = (\tilde{k}_{\sigma[\sigma]} + iZ)/\tilde{q}_\sigma$ ,  $K_2^R = (\tilde{k}_{\sigma[\sigma]} - iZ)/\tilde{q}_\sigma$ , for the P [AP] alignment. Here,  $K_1^{L*} = (\tilde{k}_\sigma - iZ)/\tilde{q}_\sigma$  is the complex conjugate of  $K_1^L$ , and  $Z = 2m\hat{W}/\hbar^2 k_F^{(S)}$  is the parameter measuring the strength of each interface barrier. Approximated wave-vector components, in units of  $k_F^{(S)}$ , are  $\tilde{q}_\sigma = \sqrt{1 - \tilde{\mathbf{k}}_{||,\sigma}^2}$ ,  $\tilde{k}_\sigma = \lambda_\sigma \cos \theta$ , and  $|\tilde{\mathbf{k}}_{||,\sigma}| = \lambda_\sigma \sin \theta$ , where  $\lambda_\sigma = \kappa \sqrt{1 + \rho_\sigma X}$ ,  $X = h_0/E_F^{(F)} \geq 0$ , and  $\kappa \neq 1$  is measuring FWVM.

In the corresponding FNF double junction, AR and TH processes are absent, and the expression for NR amplitude, Eq. (17), reduces to

$$b_\sigma^N(E, \theta) = \frac{(K_1^{L*} - K_1^R) \cos(lq_\sigma^N) + i(1 - K_1^{L*} K_1^R) \sin(lq_\sigma^N)}{(K_1^L + K_1^R) \cos(lq_\sigma^N) - i(1 + K_1^L K_1^R) \sin(lq_\sigma^N)}, \quad (21)$$

where  $q_\sigma^N = \sqrt{(2m/\hbar^2)(E_F^{(S)} + E) - \mathbf{k}_{||,\sigma}^2}$ .

To complete our considerations, we also present the probability amplitudes for an FS single junction in the same notation,

$$a_\sigma(E, \theta) = \frac{2(\tilde{k}_\sigma/\tilde{q}_\sigma)\Delta}{\mathcal{A}_+^L E + \mathcal{B}_+^L \Omega}, \quad (22)$$

$$b_\sigma(E, \theta) = \frac{\mathcal{C}_+ E + \mathcal{D}_+ \Omega}{\mathcal{A}_+^L E + \mathcal{B}_+^L \Omega}, \quad (23)$$

$$c_\sigma(E, \theta) = \frac{2(\tilde{k}_\sigma/\tilde{q}_\sigma)E\bar{u}(1 + K_2^L)}{\mathcal{A}_+^L E + \mathcal{B}_+^L \Omega}, \quad (24)$$

$$d_\sigma(E, \theta) = \frac{2(\tilde{k}_\sigma/\tilde{q}_\sigma)E\bar{v}(1 - K_2^L)}{\mathcal{A}_+^L E + \mathcal{B}_+^L \Omega}. \quad (25)$$

Note that  $c_\sigma$  and  $d_\sigma$  now describe the transmission of the Bogoliubov electron-like and hole-like quasiparticle, respectively. The well-known BTK results can be reproduced by taking  $X = 0$ ,  $\kappa = 1$ , and  $\theta = 0$  in Eqs. (22)-(25).<sup>41</sup> In case of the simplest NSN metallic junction, taking  $X = 0$ ,  $Z = 0$ , and  $\kappa = 1$  in Eqs. (16)-(19), the scattering probabilities can be written in an explicit form<sup>36</sup>

$$A_\sigma(E, \theta) = \left| \frac{\Delta \sin(\zeta_-/2)}{E \sin(\zeta_-/2) + i\Omega \cos(\zeta_-/2)} \right|^2, \quad (26)$$

$$B_\sigma(E, \theta) = D_\sigma(E, \theta) = 0, \quad (27)$$

$$C_\sigma(E, \theta) = \left| \frac{\Omega}{E \sin(\zeta_-/2) + i\Omega \cos(\zeta_-/2)} \right|^2. \quad (28)$$

Solutions for the other three types of injection can be obtained by the same procedure. In particular, if a hole with energy  $-E$ , spin  $\sigma$ , and angle of incidence  $\theta$  is injected from the left, the substitution  $q_\sigma^+ \Rightarrow q_\sigma^-$  holds, and the scattering probabilities are the same as for the injection of an electron with  $E$ ,  $\sigma$ , and  $\theta$ . Therefore, in order to include the description of both electron and hole injection, the calculated probabilities should be regarded as even functions of  $E$ . Also, for an electron or a hole, injected from the right, the probabilities are the same as for the injection from the left, except  $\sigma \rightarrow \bar{\sigma}$  for the AP alignment.

Following the conservation of  $\mathbf{k}_{\parallel,\sigma}$ , transmission of an electron (hole) with  $\sigma = \uparrow$ , injected from the left electrode into the superconductor, is possible only for angles of incidence  $\theta$  satisfying  $\theta < \theta_{c1}$ , where  $\theta_{c1} = \arcsin(1/\lambda_\uparrow)$  is the angle of total reflection. Then,  $A_\uparrow(E, \theta) = 0$  and  $B_\uparrow(E, \theta) = 1$  for  $\theta > \theta_{c1}$ . On the other hand,  $\tilde{k}_\downarrow$ , which corresponds to the hole (electron) created by the Andreev reflection, is real only for  $\theta < \theta_{c2} = \arcsin(\lambda_\downarrow/\lambda_\uparrow)$ . The virtual Andreev reflection occurs for  $\theta_{c2} < \theta < \theta_{c1}$ , since  $\tilde{k}_\downarrow$  becomes imaginary in that case. For injection of an electron (hole) with  $\sigma = \downarrow$ , transmission into the superconductor is possible for any  $\theta < \pi/2$ , and  $\tilde{k}_\uparrow$  is always real.<sup>9</sup>

From Eqs. (16) and (19) it follows that  $A_\sigma(E, \theta) = D_\sigma(E, \theta) = 0$  when

$$\zeta_- = 2n\pi \quad (29)$$

for  $n = 0, \pm 1, \pm 2, \dots$ . Therefore, the Andreev reflection at both interfaces vanishes at the energies of geometrical resonances in quasiparticle spectrum. The effect is similar to the over-the-barrier resonances in the simple problem of one-particle scattering against a step-function potential,<sup>42</sup> the superconducting gap playing the role of a finite-width barrier (as in the semiconductor model<sup>43</sup>). The absence of AR and TH processes means that all quasiparticles with energies satisfying Eq. (29) will pass unaffected from one electrode to another, without creation or annihilation of Cooper pairs.

Characteristic features of coherent quantum transport through clean superconducting layers are the subgap tunneling and oscillations of the scattering probabilities. For  $E < \Delta$ , the subgap tunneling suppresses the Andreev reflection, thereby enhancing the transmission. For  $E > \Delta$ , all probabilities oscillate with  $E$  and  $l$  due to the interference effect. The interface resistance reduces AR and TE, and enhances NR and TH probabilities. In contrast to the positions of zeros of  $A_\sigma(E, 0)$ , given by Eq. (29), the positions of maxima of  $A_\sigma(E, 0)$ , as well as that of zeros and maxima of  $B_\sigma(E, 0)$ ,  $C_\sigma(E, 0)$ , and  $D_\sigma(E, 0)$ , are  $Z$ -dependent. Approaching the tunnel limit ( $Z \rightarrow \infty$ ), peaks in the scattering probabilities gradually split into two spikes belonging to consecutive pairs with positions defined by the quantization conditions

$$lq_\sigma^+ = n_1\pi, \quad lq_\sigma^- = n_2\pi. \quad (30)$$

Here,  $n_1 - n_2 = 2n$ , with  $n$  corresponding to that of Eq. (29). The exception is the spike at the gap edge, originating from the singularity in the BCS density of states. Note that Eq. (30) gives the bound state energies of an isolated

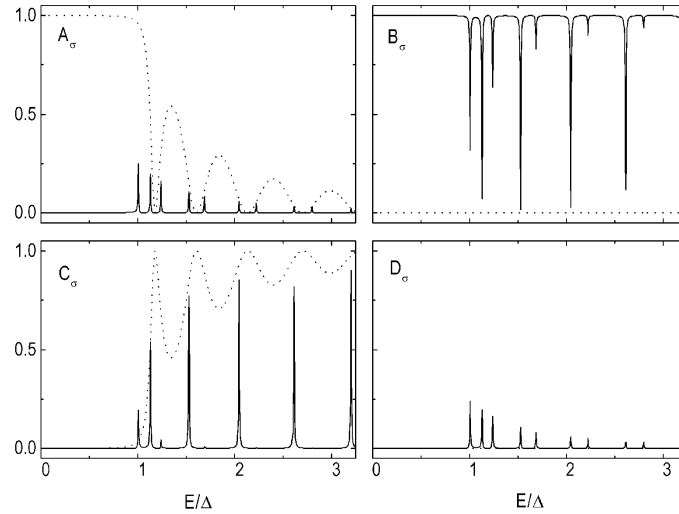


FIG. 2: Scattering probabilities,  $A_\sigma(E, 0)$ ,  $B_\sigma(E, 0)$ ,  $C_\sigma(E, 0)$ , and  $D_\sigma(E, 0)$ , for an NSN double junction with transparent and highly non-transparent interfaces,  $Z = 0$  (dotted curves) and  $Z = 10$  (solid curves), respectively. The parameters are  $lk_F^{(S)} = 10^4$ ,  $X = 0$ ,  $\kappa = 1$ , and  $\Delta/E_F^{(S)} = 10^{-3}$ .

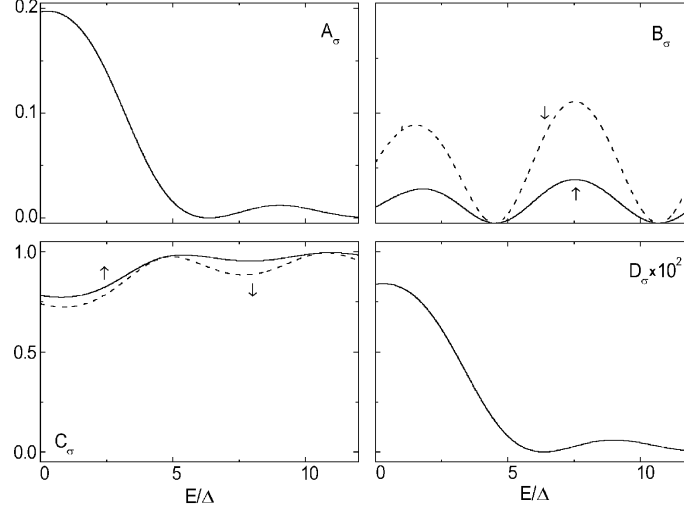


FIG. 3: Scattering probabilities,  $A_\sigma(E, 0)$ ,  $B_\sigma(E, 0)$ ,  $C_\sigma(E, 0)$ , and  $D_\sigma(E, 0)$ , for an FSF double junction with thin superconducting film,  $lk_F^{(S)} = 10^3$ , for  $X = 0.5$ ,  $Z = 0$ ,  $\kappa = 1$ ,  $\Delta/E_F^{(S)} = 10^{-3}$ , and P alignment. Solid curves: injection of an electron with  $\sigma = \uparrow$ . Dashed curves: injection of an electron with  $\sigma = \downarrow$ .

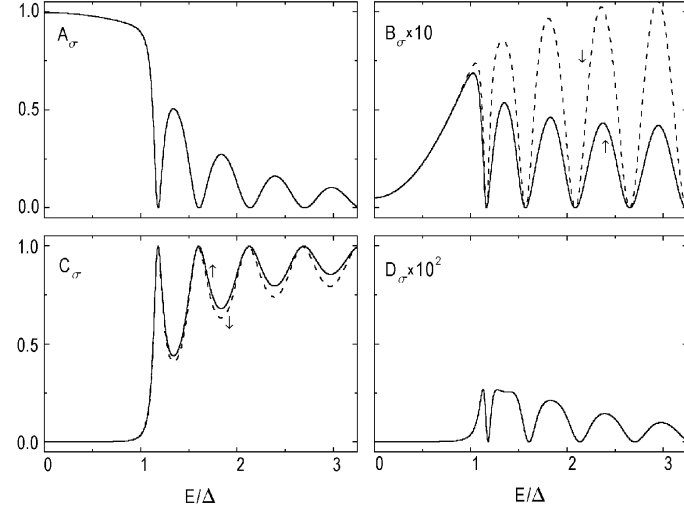


FIG. 4: Scattering probabilities,  $A_\sigma(E, 0)$ ,  $B_\sigma(E, 0)$ ,  $C_\sigma(E, 0)$ , and  $D_\sigma(E, 0)$ , for an FSF double junction with thick superconducting film,  $lk_F^{(S)} = 10^4$ , for  $X = 0.5$ ,  $Z = 0$ ,  $\kappa = 1$ ,  $\Delta/E_F^{(S)} = 10^{-3}$ , and P alignment. Solid curves: injection of an electron with  $\sigma = \uparrow$ . Dashed curves: injection of an electron with  $\sigma = \downarrow$ .

superconducting film. This is illustrated in Fig. 2 for an NSN junction, showing a simple connection between the resonances in metallic junctions ( $Z = 0$ ) and the bound states in the corresponding tunnel junctions ( $Z \rightarrow \infty$ ). The influence of exchange interaction is illustrated in Figs. 3 and 4 for an FSF double junction in P alignment with  $Z = 0$  and  $\kappa = 1$ . Taking  $\Delta/E_F^{(S)} = 10^{-3}$ , in a thin superconducting film,  $lk_F^{(S)} \sim 10^3$ , the Andreev reflection is strongly suppressed, since the subgap transmission is considerable, Fig. 3. In this case, the oscillations are less pronounced, with the period much larger than  $\Delta$ . For a thick film,  $lk_F^{(S)} \sim 10^4$ , the subgap tunneling is irrelevant (except for small 'tails' in  $A_\sigma(E, 0)$  and  $C_\sigma(E, 0)$  at  $E \lesssim \Delta$ ) and above the gap the oscillations are pronounced, with the period on the order of  $\Delta$ , Fig. 4. The scattering probabilities for AP alignment differ very slightly in the case of normal incidence,  $\theta = 0$ . Although spin-independent due to the singlet-state pairing,  $A_\sigma(E, 0)$  is suppressed in comparison with the corresponding NSN junction, and  $D_\sigma(E, 0)$  becomes non-trivial. The spin-dependent normal reflection also occurs,  $B_\sigma(E, 0)$  having zeros at the same energies as  $A_\sigma(E, 0)$  and  $D_\sigma(E, 0)$ , so that maxima in  $C_\sigma(E, 0)$  are still equal to unity due to the interface transparency.

### III. DIFFERENTIAL CONDUCTANCES

When voltage  $V$  is applied to the junction, the charge current density is given by

$$j_q(V) = \sum_{\sigma} \int \frac{d^3\mathbf{k}}{(2\pi)^3} e\mathbf{v} \cdot \hat{\mathbf{z}} \delta f(\mathbf{k}, V), \quad (31)$$

where  $\mathbf{v} = (\hbar/m)\Im[u_{\sigma}^*(\mathbf{r})\nabla u_{\sigma}(\mathbf{r}) + v_{\bar{\sigma}}^*(\mathbf{r})\nabla v_{\bar{\sigma}}(\mathbf{r})]$  is the velocity, and  $\delta f(\mathbf{k}, V)$  is the asymmetric part of the nonequilibrium distribution function of current carriers. Using the solution of the scattering problem for the injection of an electron from the left, described in the previous section, and the dispersion relation  $\mathbf{k}(E) = k_{\sigma}^+ \hat{\mathbf{z}} + \mathbf{k}_{\parallel, \sigma}$ , Eq. (31) can be rewritten in the form

$$j_q(V) = \frac{ek_F^{(S)2}}{\pi\hbar} \int_{-\infty}^{\infty} dE \sum_{\sigma} \lambda_{\sigma}^2 \int_0^{\pi/2} d\theta \sin\theta \cos\theta [1 + A_{\sigma}(E, \theta) - B_{\sigma}(E, \theta)] \delta f(\mathbf{k}, V). \quad (32)$$

In accordance with BTK, without solving the suitable transport equation, we take  $\delta f(\mathbf{k}, V) = f_0(E - eV/2) - f_0(E + eV/2)$ , where  $f_0(E)$  is the Fermi-Dirac equilibrium distribution function.

In this approach, the charge current per electron is given by

$$I_q(V) = \frac{1}{e} \int_{-\infty}^{\infty} dE [f_0(E - eV/2) - f_0(E + eV/2)] G_q(E), \quad (33)$$

where the spin-averaged differential charge conductance at zero temperature is

$$G_q(E) = \frac{e^2}{2h} \sum_{\sigma} \lambda_{\sigma}^2 \int_0^{\pi/2} d\theta \sin\theta \cos\theta [1 + A_{\sigma}(E, \theta) - B_{\sigma}(E, \theta)]. \quad (34)$$

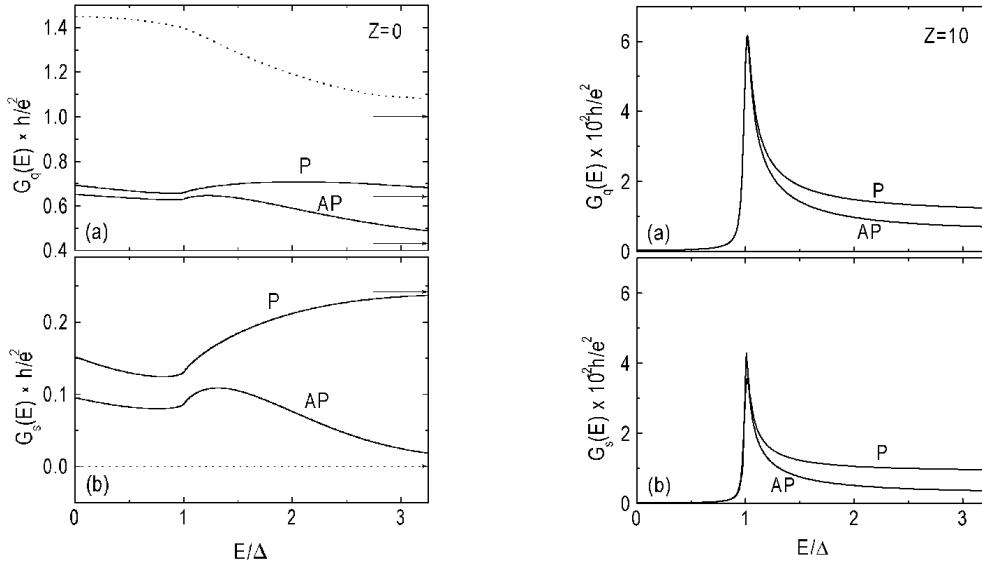


FIG. 5: **(Left panel)** Differential charge (a) and spin (b) conductance spectra,  $G_q(E)$  and  $G_s(E)$ , of an FSF double planar junction with thin superconducting film,  $lk_F^{(S)} = 10^3$ , for  $X = 0.5$ ,  $Z = 0$ ,  $\kappa = 1$ ,  $\Delta/E_F^{(S)} = 10^{-3}$ , in P and AP alignment. Conductances of the corresponding NSN junction are shown for comparison (dotted curves). Arrows indicate  $G_q^N$  and  $G_s^N$  values.

FIG. 6: **(Right panel)** Differential charge (a) and spin (b) conductance spectra,  $G_q(E)$  and  $G_s(E)$ , of an FSF double tunnel junction with thin superconducting film,  $lk_F^{(S)} = 10^3$ , for  $X = 0.5$ ,  $Z = 10$ ,  $\kappa = 1$ ,  $\Delta/E_F^{(S)} = 10^{-3}$ , in P and AP alignment.

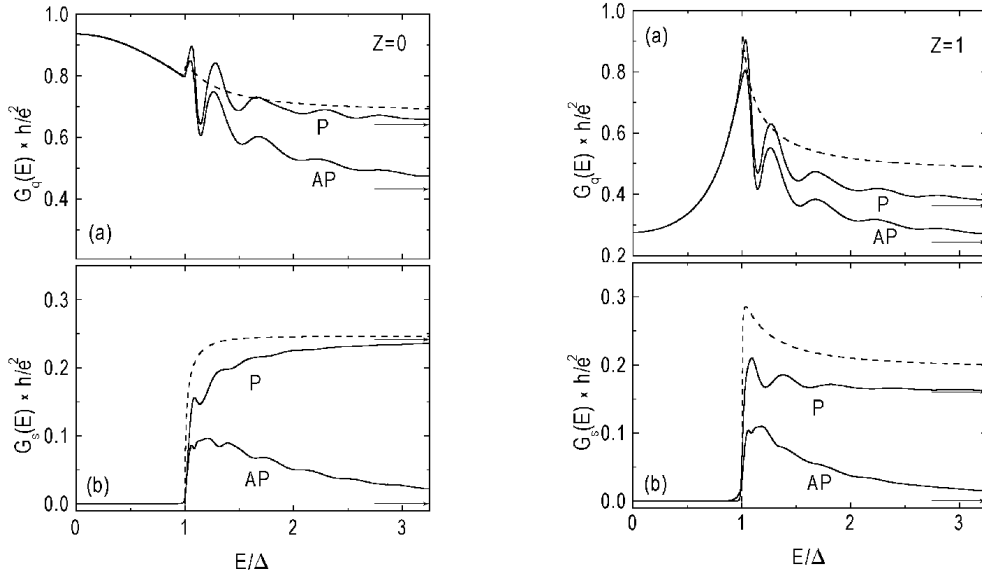


FIG. 7: **(Left panel)** Differential charge (a) and spin (b) conductance spectra,  $G_q(E)$  and  $G_s(E)$ , of an FSF double planar junction with thick superconducting film,  $lk_F^{(S)} = 10^4$ , for  $X = 0.5$ ,  $Z = 0$ ,  $\kappa = 1$ ,  $\Delta/E_F^{(S)} = 10^{-3}$ , in P and AP alignment. Dashed curves represent the generalized BTK results for the same parameters. Arrows indicate  $G_q^N$  and  $G_s^N$  values.

FIG. 8: **(Right panel)** Differential charge (a) and spin (b) conductance spectra,  $G_q(E)$  and  $G_s(E)$ , of an FSF double planar junction with thick superconducting film,  $lk_F^{(S)} = 10^4$ , for  $X = 0.5$ ,  $Z = 1$ ,  $\kappa = 1$ ,  $\Delta/E_F^{(S)} = 10^{-3}$ , in P and AP alignment. Dashed curves represent the generalized BTK results for the same parameters. Arrows indicate  $G_q^N$  and  $G_s^N$  values.

By analogy, the corresponding spin current (proportional to the probability current) is given by

$$I_s(V) = \frac{1}{e} \int_{-\infty}^{\infty} dE [f_0(E - eV/2) - f_0(E + eV/2)] G_s(E), \quad (35)$$

where the differential spin conductance at zero temperature is

$$G_s(E) = \frac{e^2}{2h} \sum_{\sigma} \rho_{\sigma} \lambda_{\sigma}^2 \int_0^{\pi/2} d\theta \sin \theta \cos \theta [1 - A_{\sigma}(E, \theta) - B_{\sigma}(E, \theta)]. \quad (36)$$

Note that in Eqs. (34) and (36) the upper limit of integration over  $\theta$  for  $\sigma = \uparrow$  is the angle of total reflection  $\theta_{c1} \leq \pi/2$ . Avoiding integration over  $\theta$ , the differential charge and spin conductances of a point-contact FSF double junction are simply expressed by

$$G_q(E) = \frac{e^2}{2h} \sum_{\sigma} \lambda_{\sigma}^2 [1 + A_{\sigma}(E, 0) - B_{\sigma}(E, 0)] \quad (37)$$

and

$$G_s(E) = \frac{e^2}{2h} \sum_{\sigma} \rho_{\sigma} \lambda_{\sigma}^2 [1 - A_{\sigma}(E, 0) - B_{\sigma}(E, 0)]. \quad (38)$$

The influence of the exchange interaction on the conductance spectra is shown for  $X = 0.5$  on the example of thin,  $lk_F^{(S)} = 10^3$ , and thick,  $lk_F^{(S)} = 10^4$ , superconducting films (Figs. 5-8). Besides the case of transparent interfaces,  $Z = 0$  (Figs. 5 and 7), the effect of interface resistance is illustrated in the tunnel limit,  $Z = 10$ , and for weak



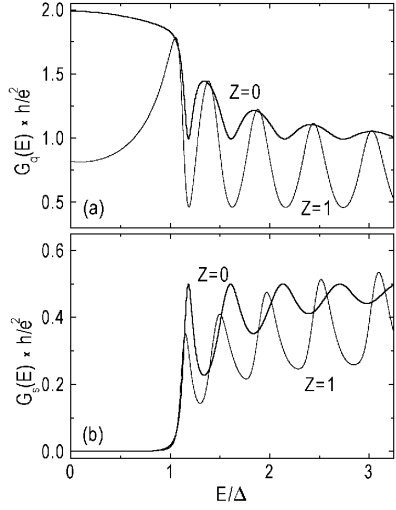


FIG. 9: **(Left panel)** Differential charge (a) and spin (b) conductance spectra,  $G_q(E)$  and  $G_s(E)$ , of a point-contact FSF double junction, with P alignment, for the same parameters as in Figs. 7 and 8 ( $X = 0.5$ ,  $\Delta/E_F^{(S)} = 10^{-3}$ ,  $lk_F^{(S)} = 10^4$ , and  $\kappa = 1$ ). Here, the difference between conductances for the AP and the P alignment is negligible.

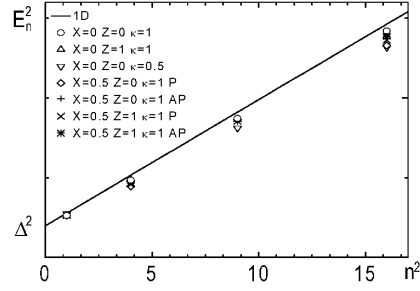


FIG. 10: **(Right panel)** Square of resonant energies  $E_n^2$  as a function of  $n^2$ , obtained from positions of minima of  $G(E)$  for  $lk_F^{(S)} = 10^4$ . The intercept is  $\Delta^2$  and the slope is  $(\hbar v_F^{(S)}/2l)^2$ .

non-transparency,  $Z = 1$ , in Figs. 6 and 8. The influence of FWVM on the conductance spectra,  $\kappa \neq 1$ , is similar to that of the interface resistance.<sup>35</sup> The values of normal conductances,  $G_q^N$  and  $G_s^N$  of the corresponding FNF double planar junction, indicated by arrows, are obtained by setting  $A_\sigma(E, \theta) = 0$  and  $B_\sigma(E, \theta) = |b_\sigma^N(E, \theta)|^2$  in Eqs. (34) and (36), where  $b_\sigma^N(E, \theta)$  is given by Eq. (21).

The spin-polarized subgap tunneling of quasiparticles, and strong suppression of the Andreev reflection as a consequence, is significant in thin superconducting films, whereas the conductance oscillations above the gap are pronounced in the thick films. The magnetoresistance is apparent, as charge and spin conductances are larger for the P than for the AP alignment. An important consequence of the coherent transport is that the spin conductance is non-trivial for the AP alignment, approaching its normal value  $G_s^N = 0$  either for  $E/\Delta \gg 1$ , or in the tunnel limit ( $Z \rightarrow \infty$ ) for all energies. We emphasize that the amplitudes of the oscillations are considerably larger for the point-contact FSF than for the planar FSF double junction, Fig. 9.

Incoherent transport through an FSF double junction is described as a transport through the corresponding FS and SF junctions in series. In that case, the conductance spectra are calculated using the generalized BTK probabilities, obtained from Eqs. (22) and (23). Numerical results for the incoherent transport are also presented in Figs. 7 and 8 for comparison. It is evident that in thick films the only difference comes from the interference-effect oscillations for the energies above the gap. In contrast with the coherent transport, for the AP alignment  $G_s(E) \equiv 0$ , and nonequilibrium spin density accumulation changes the chemical potential of two spin subbands in the superconductor. This reduces the superconducting gap with increasing voltage, and destroys the superconductivity at a critical voltage on the order of  $\Delta/e$ .<sup>23</sup> The effect of incoherency is less pronounced in metallic than in the tunnel junctions due to the Andreev reflection.<sup>24</sup>

The results can be applied to reliable spectroscopic measurements of  $\Delta$  and  $v_F^{(S)}$  in superconducting films. From Eq. (29), for  $\theta = 0$ , the energy  $E_n$  of the  $n$ -th geometrical resonance (conductance minimum) satisfies a simple relation

$$E_n^2 = \Delta^2 + \left( \frac{\hbar v_F^{(S)}}{2l} \right)^2 n^2. \quad (39)$$

Therefore, the linear plot of  $E_n^2$  vs  $n^2$  has the intercept equal to  $\Delta^2$  and the slope equal to  $(\hbar v_F^{(S)}/2l)^2$ . An example is shown in Fig. 10. Note that even the points obtained for planar (3D) double junctions lie almost on the same straight line given by Eq. (39) for the particular case of a point-contact (1D) double junction. The numerical results show that the method is almost independent on dimensionality of the junction and on parameters of the electrodes. The net spin polarization of the current is defined as  $\Pi(V) = I_s(V)/I_q(V)$ . In thin superconducting films,  $\Pi(V)$  is almost constant, considerably smaller than  $X$ , which is the polarization in the corresponding FNF junction. Below

the gap,  $eV/2\Delta < 1$ , the contribution of subgap tunneling to spin polarization becomes negligibly small for large  $l$ . Above the gap,  $eV/2\Delta > 1$ , the polarization increases with  $V$ , the increase becoming steeper with the interface non-transparency, Fig. 11. On the other hand, in a tunnel FS junction the polarization abruptly changes from  $\Pi = 0$  to  $\Pi = X$  at  $eV/2\Delta = 1$ . The same result holds for incoherent transport through an FSF double tunnel junction.

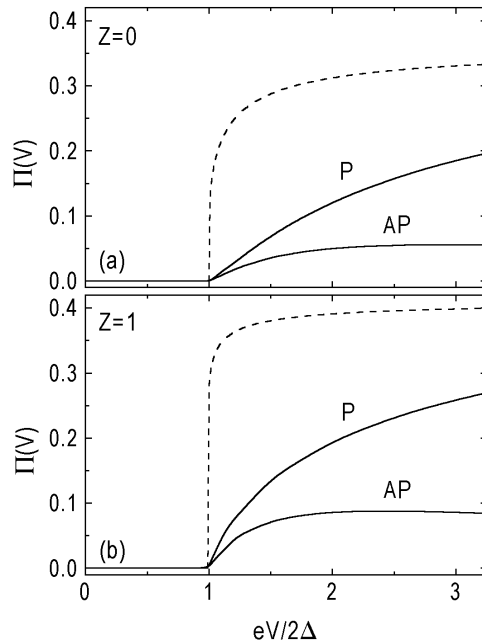


FIG. 11: Spin polarization of the current,  $\Pi(V)$ , for an FSF double planar junction with P and AP alignment, is shown for (a)  $Z = 0$ , and (b)  $Z = 1$ . Other parameters are the same as in Figs. 7 and 8 ( $X = 0.5$ ,  $\Delta/E_F^{(S)} = 10^{-3}$ ,  $lk_F^{(S)} = 10^4$ , and  $\kappa = 1$ ). Dashed curves represent the generalized BTK results.

#### IV. SUMMARY

We have analyzed transport properties of FSF double-barrier junctions, taking into account the influence of the exchange interaction, the resistance of the interfaces, and the Fermi velocity mismatch on the scattering probabilities and the conductance spectra. We have shown that subgap tunneling and oscillations of differential conductances are the main features of the coherent quantum transport through a superconducting layer in both FSF and NSN double-barrier junctions. The subgap tunneling suppresses the Andreev reflection, thereby enhancing the transmission, especially in thin films. The scattering probabilities and conductances oscillate as a function of the layer thickness and of the quasiparticle energy above the gap.

Periodic vanishing of the Andreev reflection at the energies of geometrical resonances is found as an important consequence of the quasiparticle interference. Insulating barriers at the interfaces reduce the Andreev reflection and transmission, mainly for energies below the gap. The Fermi velocity mismatch has a similar effect. Results are directly accessible to experiments. In principle, oscillations of differential conductances with the period of geometrical resonances could be used for reliable spectroscopy of quasiparticle excitations in superconductors.

In conclusion, finite-size effects, along with the difference between coherent and incoherent transport, are essential for spin-currents in FSF junctions. For the coherent transport, besides the spin-polarized subgap tunneling in thin superconducting films, pronounced oscillations of spin conductance occur in thick films. As a consequence of the quasiparticle interference, a non-trivial spin current without the excess spin accumulation and destruction of superconductivity is possible even for AP alignment of the electrode magnetizations.

## V. ACKNOWLEDGMENT

We are grateful to Ivan Božović for pointing out the significance of the problem treated in this paper, and for help at the initial stage of this work. Furthermore, we thank Irena Knežević for useful discussions. This work has been supported by the Serbian Ministry of Science, Technology, and Development, grant N°1899.

- 
- <sup>1</sup> G. A. Prinz, Phys. Today **48** (4), 58 (1995).
  - <sup>2</sup> M. Osofsky, J. Supercond. **13**, 209 (2000).
  - <sup>3</sup> G. E. Blonder, M. Tinkham, and T. M. Klapwijk, Phys. Rev. B **25**, 4515 (1982).
  - <sup>4</sup> A. F. Andreev, Zh. Éksp. Teor. Fiz. **46**, 1823 (1964) [Sov. Phys. JETP **19**, 1228 (1964)].
  - <sup>5</sup> A. Furusaki and M. Tsukada, Solid State Commun. **78**, 299 (1991).
  - <sup>6</sup> Y. Tanaka and S. Kashiwaya, Phys. Rev. Lett. **74**, 3451 (1995).
  - <sup>7</sup> S. Kashiwaya and Y. Tanaka, Rep. Prog. Phys. **63**, 1641 (2000).
  - <sup>8</sup> M. J. M. de Jong and C. W. J. Beenakker, Phys. Rev. Lett. **74**, 1657 (1995).
  - <sup>9</sup> S. Kashiwaya, Y. Tanaka, N. Yoshida, and M. R. Beasley, Phys. Rev. B **60**, 3572 (1999).
  - <sup>10</sup> N. Yoshida, Y. Tanaka, J. Inoue, and S. Kashiwaya, J. Phys. Soc. Jpn. **68**, 1071 (1999).
  - <sup>11</sup> I. Žutić and O. T. Valls, Phys. Rev. B **60**, 6320 (1999).
  - <sup>12</sup> J.-X. Zhu, B. Friedman, and C. S. Ting, Phys. Rev. B **59**, 9558 (1999).
  - <sup>13</sup> P. M. Tedrow and R. Meservey, Phys. Rep. **238**, 173 (1994).
  - <sup>14</sup> C. L. Platt, A. S. Katz, E. P. Price, R. C. Dynes, and A. E. Berkowitz, Phys. Rev. B **61**, 68 (2000).
  - <sup>15</sup> R. J. Soulen Jr. *et al.*, Science **282**, 85 (1998).
  - <sup>16</sup> G. J. Strijkers, Y. Ji, F. Y. Yang, C. L. Chien, and J. M. Byers, Phys. Rev. B **63**, 104510 (2001).
  - <sup>17</sup> S. K. Upadhyay, A. Palanisami, R. N. Louie, and R. A. Buhrman, Phys. Rev. Lett. **81**, 3247 (1998).
  - <sup>18</sup> V. A. Vas'ko, K. R. Nikolaev, V. A. Larkin, P. A. Kraus, and A. M. Goldman, App. Phys. Lett. **73**, 844 (1998).
  - <sup>19</sup> F. J. Jedema, B. J. van Wees, B. H. Hoving, A. T. Filip, and T. M. Klapwijk, Phys. Rev. B **60**, 16 549 (1999).
  - <sup>20</sup> S. Guéron, H. Pothier, N. O. Birge, D. Esteve, and M. H. Devoret, Phys. Rev. Lett. **77**, 3025 (1996).
  - <sup>21</sup> V. T. Petrashov, I. A. Sosnin, I. Cox, A. Parsons, and C. Troadec, J. Low Temp. Phys. **118**, 689 (2000).
  - <sup>22</sup> M. A. Sillanpää, T. T. Heikkilä, R. K. Lindell, and P. J. Hakonen, cond-mat/0102367 (unpublished).
  - <sup>23</sup> S. Takahashi, H. Imamura, and S. Maekawa, Phys. Rev. Lett. **82**, 3911 (1999).
  - <sup>24</sup> Z. Zheng, D. Y. Xing, G. Sun, and J. Dong, Phys. Rev. B **62**, 14326 (2000).
  - <sup>25</sup> M. Zareyan, W. Belzig, and Yu. V. Nazarov, Phys. Rev. Lett. **86**, 308 (2001).
  - <sup>26</sup> T. M. Klapwijk, G. E. Blonder, and M. Tinkham, Physica B **109-110**, 1657 (1982).
  - <sup>27</sup> T. Hoss, C. Strunk, T. Nussbaumer, R. Huber, U. Staufer, and C. Schönenberger, Phys. Rev. B **62**, 4079 (2000).
  - <sup>28</sup> Å. Ingeman, G. Johansson, V. S. Shumeiko, and G. Wendin, Phys. Rev. B **64**, 144504 (2001).
  - <sup>29</sup> W. J. Tomasch, Phys. Rev. Lett. **15**, 672 (1965); *ibid.* **16**, 16 (1966).
  - <sup>30</sup> W. L. McMillan and P. W. Anderson, Phys. Rev. Lett. **16**, 85 (1966).
  - <sup>31</sup> J. M. Rowell and W. L. McMillan, Phys. Rev. Lett. **16**, 453 (1966).
  - <sup>32</sup> W. L. McMillan, Phys. Rev. **175**, 559 (1968).
  - <sup>33</sup> J. Demers and A. Griffin, Can. J. Phys. **49**, 285 (1971).
  - <sup>34</sup> O. Neshor and G. Koren, Phys. Rev. B **60**, 9287 (1999).
  - <sup>35</sup> M. Božović and Z. Radović, Phys. Rev. B, submitted (2002).
  - <sup>36</sup> M. Božović, Z. Pajović, and Z. Radović, Physica C, submitted (2002).
  - <sup>37</sup> J. M. E. Geers, M. B. S. Hesselberth, J. Aarts, and A. A. Golubov, Phys. Rev. B **64**, 094506 (2001).
  - <sup>38</sup> I. Baladié, A. Buzdin, N. Ryzhanova, and A. Vedyayev, Phys. Rev. B **63**, 054518 (2001).
  - <sup>39</sup> V. I. Fal'ko, A. F. Volkov, and C. Lambert, Phys. Rev. B **60**, 15394 (1999).
  - <sup>40</sup> E. McCann, V. I. Fal'ko, A. F. Volkov, and C. J. Lambert, Phys. Rev. B **62**, 6015 (2000).
  - <sup>41</sup> The parameter  $Z$  in our definition differs from the BTK by a factor of 2.
  - <sup>42</sup> C. Cohen-Tannoudji, B. Diu, and F. Laloe, *Quantum Mechanics*, (Hermann, Paris, 1977).
  - <sup>43</sup> M. Tinkham, *Introduction to Superconductivity*, (McGraw-Hill, New York, 1996).